Title

Multilineage somatic activating mutations in HRAS and NRAS cause mosaic cutaneous and skeletal lesions, elevated FGF23 and hypophosphatemia.

Journal

Human molecular genetics, 23(2)

ISSN

0964-6906

Authors

Lim, Young H

Ovejero, Diana

Sugarman, Jeffrey S

et al.

Publication Date

2014

DOI

10.1093/hmg/ddt429

Peer reviewed

Human Molecular Genetics, 2014, Vol. 23, No. 2 **397–407**
doi:10.1093/hmg/ddt429
Advance Access published on September 4, 2013

Multilineage somatic activating mutations in *HRAS* and *NRAS* cause mosaic cutaneous and skeletal lesions, elevated FGF23 and hypophosphatemia

Young H. Lim[1], Diana Ovejero[4,7], Jeffrey S. Sugarman[8,9], Cynthia M.C. DeKlotz[10,12,13], Ann Maruri[14,15], Lawrence F. Eichenfield[10,12,13], Patrick K. Kelley[17], Harald Jüppner[18], Michael Gottschalk[11,14], Cynthia J. Tifft[19,5], Rachel I. Gafni[4], Alison M. Boyce[4,20], Edward W. Cowen[6], Nisan Bhattacharyya[4], Lori C. Guthrie[4], William A. Gahl[19,5], Gretchen Golas[19,5], Erin C. Loring[2,21], John D. Overton[2,21], Shrikant M. Mane[2,21], Richard P. Lifton[2,21,3], Moise L. Levy[16,22,23,24], Michael T. Collins[4,*] and Keith A. Choate[1,*]

[1]Department of Dermatology, [2]Department of Genetics and [3]Howard Hughes Medical Institute, Yale University School of Medicine, New Haven, CT 06510, USA [4]Skeletal Clinical Studies Unit, Craniofacial and Skeletal Disease Branch, National Institute of Dental and Craniofacial Research, [5]Office of the Clinical Director, NHGRI and [6]Dermatology Branch, Center for Cancer Research, National Cancer Institute, National Institutes of Health, Bethesda, MD 20892, USA [7]Departament de Medicina, Universitat Autònoma de Barcelona, Bellaterra, Spain [8]Department of Dermatology [9]Department of Family Medicine, University of California, San Francisco, San Francisco, CA 95403, USA [10]Division of Pediatric and Adolescent Dermatology and [11]Pediatric Endocrinology, Rady Children's Hospital, San Diego, USA [12]Department of Pediatrics and [13]Department of Medicine (Dermatology), University of California, San Diego, CA 92123, USA [14]Pediatric Care of Ogden, Ogden, UT, USA [15]College of Nursing, University of Utah, Salt Lake City, UT 84112, USA [16]Pediatric and Adolescent Dermatology and [17]Seton Institute of Reconstructive Plastic Surgery, University Medical Center Brackenridge, Dell Children's Medical Center of Central Texas, Austin, TX 78723, USA [18]Pediatric Nephrology Unit and Endocrine Unit, Massachusetts General Hospital, Harvard Medical School, Boston, MA 02114, USA [19]NIH Undiagnosed Diseases Program, NIH Common Fund, Bethesda, MD 20892, USA [20]Bone Health Program, Division of Orthopaedics and Sports Medicine, Children's National Medical Center, 111 Michigan Avenue NW, Washington, DC 20010, USA [21]Yale Center for Mendelian Genomics, New Haven, CT 06510, USA [22]Department of Dermatology, UT Southwestern Medical School, Dallas, TX, USA [23]Department of Pediatrics [24]Department of Dermatology, Baylor College of Medicine, Houston, TX 77030, USA

Received June 17, 2013; Revised August 1, 2013; Accepted August 30, 2013

Pathologically elevated serum levels of fibroblast growth factor-23 (FGF23), a bone-derived hormone that regulates phosphorus homeostasis, result in renal phosphate wasting and lead to rickets or osteomalacia. Rarely, elevated serum FGF23 levels are found in association with mosaic cutaneous disorders that affect large proportions of the skin and appear in patterns corresponding to the migration of ectodermal progenitors. The cause and source of elevated serum FGF23 is unknown. In those conditions, such as epidermal and large congenital melanocytic nevi, skin lesions are variably associated with other abnormalities in the eye, brain and vasculature. The wide distribution of involved tissues and the appearance of multiple segmental skin and bone lesions suggest that these conditions result from early embryonic somatic mutations. We report five such cases with elevated serum FGF23 and bone lesions, four with large epidermal nevi and one with a giant congenital melanocytic nevus. Exome sequencing of blood and affected skin tissue identified somatic activating

*To whom correspondence should be addressed. Tel: +1 2037853912; Fax: +1 8884807802; Email: keith.choate@yale.edu (K.A.C.); Tel: +1 3014964913; Fax: +1 3014809962; Email: mcollins@dir.nidcr.nih.gov (M.T.C.)

mutations of *HRAS* or *NRAS* in each case without recurrent secondary mutation, and we further found that the same mutation is present in dysplastic bone. Our finding of somatic activating *RAS* mutation in bone, the endogenous source of FGF23, provides the first evidence that elevated serum FGF23 levels, hypophosphatemia and osteomalacia are associated with pathologic Ras activation and may provide insight in the heretofore limited understanding of the regulation of FGF23.

INTRODUCTION

Skin and skeletal lesions appearing in localized patterns are generally mosaic disorders that result from embryonic somatic mutations (1–3). The distribution and pattern of lesions are determined by the type of progenitor cell affected and the timing of mutation during embryogenesis (1,2). Epidermal nevi and congenital melanocytic nevi (EN and CMN) appear in a wide range of sizes from small subcentimeter lesions to extensive segmental lesions affecting a large fraction of the skin surface area (4,5). While both are typically limited to the skin, in rare syndromic forms including epidermal nevus syndrome (ENS), they can be accompanied by abnormalities in other organ systems, including the eyes, brain and bone (5–8). The additional systemic abnormalities almost exclusively occur in the setting of extensive skin surface area involvement, consistent with early embryonic somatic mutation in a multipotent progenitor (6–8). Since somatic mutations can occur at any point post-fertilization, timing determines the relative potential of the affected cell (9,10). Mutations prior to germ layer specification, for example, could result in progeny capable of ectodermal, mesodermal or endodermal fates as is postulated to occur in ENS (11). Later embryonic mutations affect cells with more limited potential, and thus tend to be smaller and involve a single germ layer as in the skin limited form of EN and NS (11,12).

EN, nevus comedonicus and giant CMN have been found in association with precocious puberty, cognitive dysfunction, arterial stenosis and skeletal malformations (7,13–15). Depending on the combination of cutaneous lesions and associated abnormalities, various nomenclatures such as Schimmelpenning–Feuerstein–Mims syndrome (16,17), Becker's nevus syndrome (18) and ENS have been applied, but these disorders have significant clinical overlap, suggesting a common pathogenesis.

Hypophosphatemic rickets rarely occurs in EN (27 reported cases) and CMN (1 case) (14,19–39). All reported affected individuals had skin lesions over 10–60% of the body surface area with involvement of other organ systems variably reported. In addition, each exhibited skeletal dysplasia, and in all cases in which it was assessed, low levels of blood phosphate, phosphaturia and elevated blood fibroblast growth factor-23 (FGF23) (26,32,35). FGF23 is a bone-derived hormone that regulates phosphorus homeostasis and vitamin D metabolism at the level of the renal proximal tubule cell by reducing expression of sodium-phosphate cotransporters types IIa and IIc (NPT2a, NPT2c), inhibiting 1-alpha hydroxylase activity, and enhancing 24-hydroxylase activity (40,41). Thus both renal phosphate reabsorption and synthesis of 1,25 $(OH)_2$ vitamin D3, which mediates the gastrointestinal absorption of phosphate, are impaired by elevated FGF23, collectively contributing to the development of rickets and osteomalacia (40,42). In the reported cases of hypophosphatemic rickets with skin lesions, skin involvement was widespread and abnormalities in other organ systems were frequently identified (14,27,28,30,33,36). Given the broad spectrum of cutaneous and systemic findings, we have designated this disorder cutaneous-skeletal hypophosphatemia syndrome (CSHS). The generally large size of these skin lesions and presence of systemic findings are consistent with a shared origin from an early somatic mutation.

Isolated and syndromic keratinocytic and sebaceous nevi, as well as melanocytic nevi have been shown to result from somatic activating mutations in codons 12, 13 and 61 of *RAS* gene family members, which cause cell proliferation via the MAP kinase pathway (43–46). Skin lesions from one case of Schimmelpenning syndrome with hypophosphatemic rickets were also found to have somatic activating mutations in *HRAS* (47). The Mendelian forms of hypophosphatemic rickets typically present in childhood and can be transmitted in an autosomal dominant, recessive or X-linked fashion (48–51). Almost all feature either elevated FGF23 or inappropriately normal FGF23 levels in the setting of hypophosphatemia. Autosomal dominant hypophosphatemic rickets results from missense mutations in *FGF23* that affect the C-terminal RTHR cleavage site, blocking degradation and leading to increased circulating FGF23 levels (51). X-linked hypophosphatemia is caused by inactivating mutations in the endopeptidase-encoding *PHEX* gene (49), while autosomal recessive hypophosphatemic rickets 1 and 2 (ARHR1, ARHR2) result from mutations in *DMP1* and *ENPP1*, respectively (48,50). Reports of activating mutations in FGF receptor 1 (*FGFR1*), as well as a single *de novo* translocation causing increased circulating levels of cleaved α-Klotho, a cofactor for FGF23 binding to FGFR1 in the renal tubules, have also been found to increase levels of FGF23 resulting in hypophosphatemic rickets (52,53).

The etiology of hypophosphatemia in the setting of skin lesions has remained unknown. Some reports have described improvement of phosphate homeostasis upon destruction of skin lesions via excision or ablative techniques, suggesting the skin to be a source of a phosphatonin (19,28,54). However, qRT–PCR using RNA extracted from affected skin did not demonstrate FGF23 expression in the skin, suggesting that the skin-derived phosphatonin may be an unknown substance or that the excess FGF23 is produced elsewhere (32). Others have postulated that the focal bone lesions may be the source of FGF23 in ENS (25). We have employed exome and Sanger sequencing of blood and tissue samples from a cohort of five patients, to determine the genetic mechanism of the pathophysiology of CSHS.

RESULTS

To identify the genetic basis of hypophosphatemia, elevated FGF23 levels, osteomalacia and skin lesions in CSHS, we investigated five such cases, four with EN affecting multiple

Table 1. Elevated FGF23 and hypophosphatemia in the CSHS patient cohort

Patient	Cutaneous findings	Age	Sex	FGF23 (RU/ml)	Phosphate (mg/dl)	Calcium (mg/dl)	ALKP (U/l)	PTH (pg/ml)
CSHS101	EN	5	F	276	2.0	9.1	007000	45.5
CSHS102	EN	12	F	279	2.3	9.7	003660	47.4
CSHS103	EN	15	F	527	1.5	9.3	006510	90.0[b]
CSHS104	Giant CMN	4	F	795	1.5	8.5	01081	88.5[b]
CSHS105	EN	16	M	104.5[a]	2.2	8.7	003460	47.9

Cutaneous findings, age at time of reported laboratory values, sex and values confirming the diagnosis of CSHS are presented. All patients show elevated FGF23, hypophosphatemia, normocalcemia, elevated alkaline phosphatase (ALKP) and normal 25(OH)D (calcidiol). 1,25(OH)2D (calcitriol) levels are not shown since they were confounded by the concomitant treatment with oral calcitriol. Tubular reabsorption of phosphate (TRP%) values ranged from 73 to 85.7%, consistent with renal phosphate wasting.

Reference normal values: FGF23, average for <18 years: 25–140 RU/ml; phosphate: 3.0–4.5 mg/dl; calcium: 9.0–10.5 mg/dl; alkaline phosphatase (ALKP): 30–120 U/l; parathyroid hormone (PTH), 10–60 pg/ml (115–117).

[a]CSHS105 had the intact FGF-23 measured, which is recorded in pg/ml, rather than the intact + C-terminal FGF-23, measured in RU/ml. The normal range of intact FGF-23 is 8–54 pg/ml.

[b]CSHS103 and 104 presented with low vitamin D when values were measured. Given their normal calcium levels, the elevated PTH represents secondary hyperparathyroidism, the normal physiological response to low vitamin D.

developmental segments of the skin and a single case with a giant CMN (Table 1, Fig. 1). All cases exhibited skeletal findings that included foci of dysplastic bone and fractures; most had rickets, and available lesional bone tissue demonstrated osteomalacia (Fig. 2). Histologic examination of dysplastic bone revealed fibroblast-like spindle-shaped cells surrounded by a relatively dense collagen matrix, an appearance consistent with cells in the osteogenic lineage (Fig. 3). In addition, pathologic lesions were observed in other tissues (Supplementary Material, Fig. S1). Affected individual CSHS101 had a brainstem lipoma, a thyroid nodule and splenic hemangiomas; CSHS102 manifested subaortic valve stenosis; CSHS103 had an eccrine poroma; CSHS104 displayed a left intraventricular choroidal mass and a non-pigmented mass in the medial canthus of the right eye; CSHS105 had brain abnormalities including colpocephaly and periventricular white matter paucity. These findings were consistent with somatic mosaicism for mutations contributing to multisystem disease.

Exome sequencing was performed on DNA samples from affected skin and peripheral blood leukocytes of individuals CSHS101, 102, 103 and 105, and on DNA extracted from archival affected skin from CSHS104 (Supplementary Material, Table S1). Genetic variants were annotated and compared with identify somatic mutations present solely within affected tissue and not in germline (blood) DNA. In the four samples with matched blood and skin lesion DNA, we found a single heterozygous somatic mutation, in each case a known activating mutation in either *HRAS* or *NRAS* (55–63). In addition, we found a known activating RAS mutation in the lesion that did not have matched blood DNA; in this case, the mutation was absent in DNA prepared from normal bone marrow, demonstrating its somatic origin. The mutations included c.182A>G, p.Q61R in *NRAS*; c.182A>G, p.Q61R in *HRAS*; c.37G>C, p.G13R in *HRAS* (Table 2). All these mutations were confirmed by direct Sanger sequencing (Supplementary Material, Fig. S2). No germline mutations were found in other genes implicated in congenital disorders of phosphate metabolism (*FGF23*, *FGFR1*, *FGF2*, *FGF7*, *DMP1*, *DMP4*, *ENPP1*, *KL*, *MEPE*, *PHEX*, *SLC34A1*, *SLC34A3*, *CLCN5*, *VDR*, *OPN*, *SFRP4*, *GALNT3* and *GALNT8* genes) (64–98). Furthermore, germline samples were searched for genes harboring novel protein-altering variants in more than one subject, and none were found (see Materials and Methods). Finally, plots of differences in B-allele frequency between tumor and blood did not deviate from 0.5 across the genome, excluding large segments with loss of heterozygosity in tissue (Supplementary Material, Fig. S3). Collectively, these findings suggest that somatic *RAS* mutation alone is sufficient to cause CSHS.

To further examine the etiology of elevated FGF23 and hypophosphatemia in CSHS patients, we examined dysplastic bone from cases CSHS102 and CSHS104 using Sanger sequencing, and found the same *HRAS* G13R and *NRAS* Q61R mutations present in the patients' EN and CMN, respectively. The mutations were absent in normal bone (Fig. 4). While nevus tissue of individual CSHS 104 was strongly positive via immunohistochemical staining for MelanA, a transmembrane protein expressed by melanocytes, the dysplastic bone tissue was MelanA negative, confirming that it arose independently (Fig. 5).

Given prior reports suggesting the skin lesions could be a source of elevated serum FGF23 in CSHS, we next examined affected skin tissue from four cases in our cohort (101,102,103,104) for FGF23 expression using immunohistochemical staining. Immunostaining was performed using normal skin as a negative control and a tumor-induced osteomalacia (TIO) sample as a positive control. In addition, a sporadic nevus sebaceus sample arising from a somatic *HRAS* G13R mutation was examined (45). None of the skin samples demonstrated expression of FGF23, while the TIO specimen demonstrated strongly positive staining (Supplementary Material, Fig. S4).

DISCUSSION

We have described a cohort of five cases of hypophosphatemia, skeletal dysplasia with osteomalacia and cutaneous lesions in developmental mosaic patterns, accompanied by various associated clinical findings. We define CSHS as a multisystem skin-bone disorder in which all patients have elevated circulating levels of FGF23. Further, we present the first exome sequencing analysis of CSHS in which we identified somatic activating *RAS* mutations in skin lesions of all five cases and in affected dysplastic bone of two subjects.

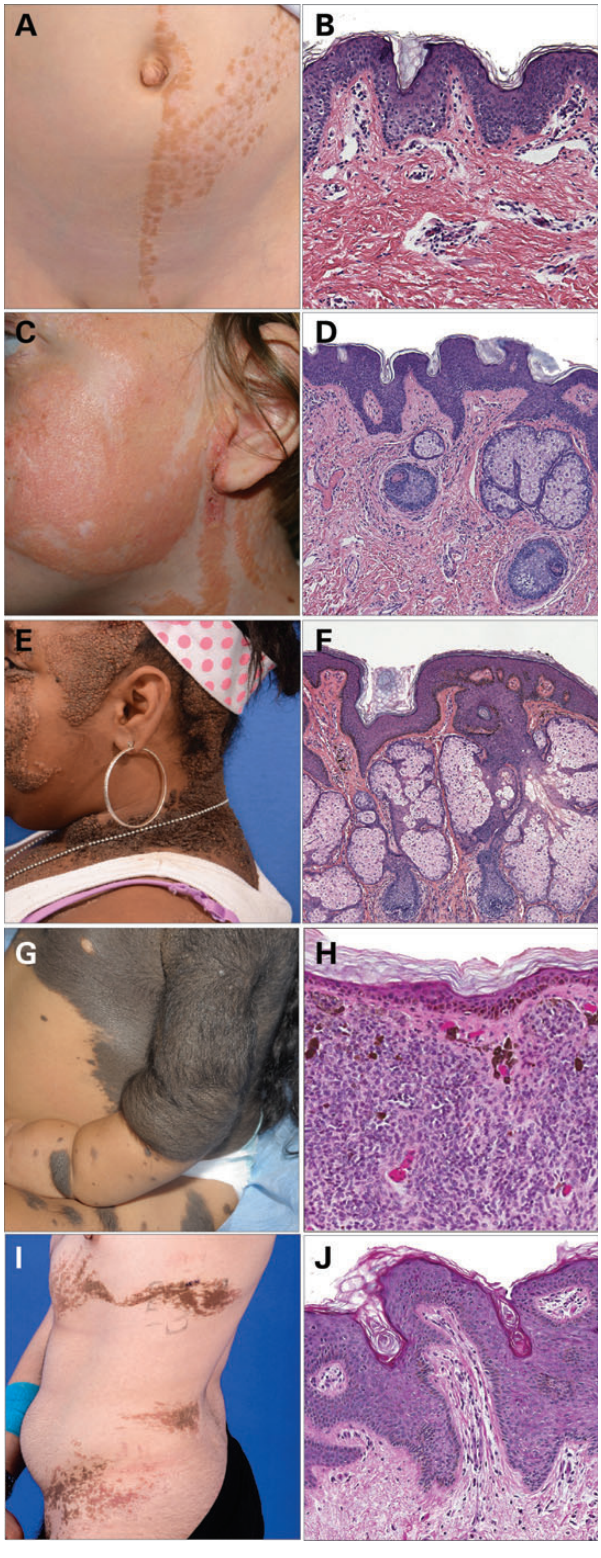

Figure 1. Clinical and histological features of CSHS. All photomicrographs are at ×10 magnification. (**A** and **B**) Affected individual CSHS101 is a 7-year-old Caucasian female who presented at birth with linear epidermal nevi restricted to the left side of her body distributed from the neck to the calf. Histopathology shows thickening of the epidermis (acanthosis) and papillomatosis. (**C** and **D**) CSHS102 is a 12-year-old Caucasian female with nevus sebaceus on the left side of her head and neck. Histology of lesional skin from the cheek shows sebaceous hyperplasia, thickening of the stratum corneum (hyperkeratosis) and papillomatosis. (**E** and **F**) CSHS103 is a 15-year-old black female with widespread keratinocytic epidermal nevi on the torso and sebaceous nevi on the scalp and cheek, with brown verrucous papules and plaques covering the scalp, face, torso and extremities, as well as linear white plaques on the scalp and torso. Histological examination shows marked sebaceous hyperplasia, hyperkeratosis and papillomatosis. (**G** and **H**) CSHS104 is a black female who presented with a giant melanocytic nevus covering the entire posterior torso at birth, extending across the flanks to the anterior chest. Round, raised, hairy and pigmented plaques determined to be satellitosis of the congenital nevi were located on her extremities. There was a 0.5 × 12 cm linear tan epidermal nevus on the left forearm (not shown). Histology of tissue from her back tissue shows melanocytes infiltrating the full thickness of the dermis, melanin deposition and hyperkeratosis. She died at 4 years of age from a large pericardial effusion that occurred during sedation for an MRI. (**I** and **J**) CSHS105 is a 16-year-old Caucasian male born with whorls of raised pink to tan plaques across the central right chest and nipple, as well as lesions extending around the flank towards the right back, all consistent with keratinocytic epidermal nevi. Histology of lesions shows hyperkeratosis, acanthosis and papillomatosis.

A similar pattern of mosaicism is found in McCune–Albright syndrome (MAS), a condition in which affected individuals demonstrate elevated FGF23, focal dysplasia of the bone, and cutaneous café-au-lait lesions (99,100). Somatic activating mutations in *GNAS*, which encodes the signaling protein $G_s\alpha$, cause MAS and have been found in the fibrous dysplasia lesions, affected skin and other affected tissues. In MAS, *in vitro* expression assays of mutant $G_s\alpha$ in osteogenic cells suggest a role for $G_s\alpha$ activation in FGF23 production and/or processing (101–105). Furthermore, just as the degree of clinical findings in MAS are dependent on the developmental timing and location of the postzygotic *GNAS* mutation during embryogenesis, the timing and location of the postzygotic *RAS* mutation in CSHS may determine the type, extent and distribution of mutated progeny cells in the body, and thus the spectrum of clinical phenotypes. Our data suggest that other rare clinical findings in patients with congenital nevi may also be attributable to somatic *RAS* mutations.

Our discovery of recurrent activating *RAS* mutations in tissues derived from different germ layers provides evidence that embryonic mutations in a common progenitor of skin and bone lead to CSHS, and suggests that the extracutaneous findings in CSHS and other ENS s result from the pleiotropic effects of *RAS* mutations acting in different tissues. Similar to postzygotic *RAS* mutations in a multipotent progenitor giving rise to both sebaceous and melanocytic nevi in phacomatosis pigmentokeratotica, *RAS* mutations found in CSHS are likely acquired during early embryogenesis in a cell destined to differentiate into both the skeletal and cutaneous systems (106). The absence of additional intersecting mutations in the exome data from our index cases and the presence of an activating *RAS* mutation in bone suggest that an activating *RAS* mutation is sufficient to drive hypophosphatemic rickets via increased production of FGF23. Support for the role of Ras in FGF23 regulation includes recent findings in a pre-osteoblast cell line and primary cultures of bone marrow stromal cells, which show that Ras is activated in response to hyperphosphatemia, an established stimulus for FGF23 secretion *in vivo* (107–109). Further support for the role of *RAS* mutations in FGF23 regulation is the recent finding of an activating somatic *KRAS* mutation (G12V) in a hepatic metastasis of an adenocarcinoma that was accompanied by elevated FGF23 levels and showed FGF23 expression on

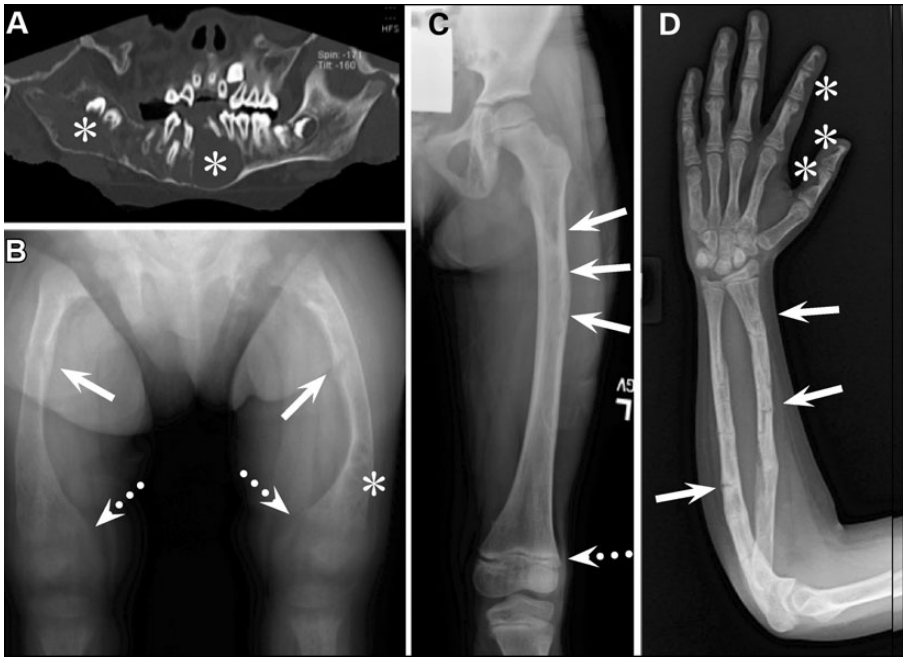

Figure 2. Radiographic features of CSHS. (**A**) A CT scan of the jaw of patient CSHS103 shows large areas of dysplastic bone (asterisks) that appear as lytic lesions. The skeletal disease in the mandible displays an aggressive expansion that displaces and resorbs the tooth roots. (**B**) A radiograph of the femurs of patient CSHS104 demonstrates healing fractures due to osteomalacic bone (solid arrows), evidence of rickets (ill-defined, frayed and widened growth plates, dotted arrows), and dysplastic bone with mixed lytic and sclerotic changes (asterisk). (**C**) A radiograph of the femur of patient CSHS101 at age 7 reveals a stretch of dysplastic bone with a primarily sclerotic appearance at this age (solid arrows). At a younger age, the same lesion was more lytic in nature (not shown). As a result of medical therapy, the growth plate is normal, with no evidence of rickets (dotted arrows). (**D**) A radiograph of the arm of patient CSHS102 shows multiple unhealed fractures (arrows). Dysplastic lesions with lytic changes are seen in some of the phalanges (asterisks).

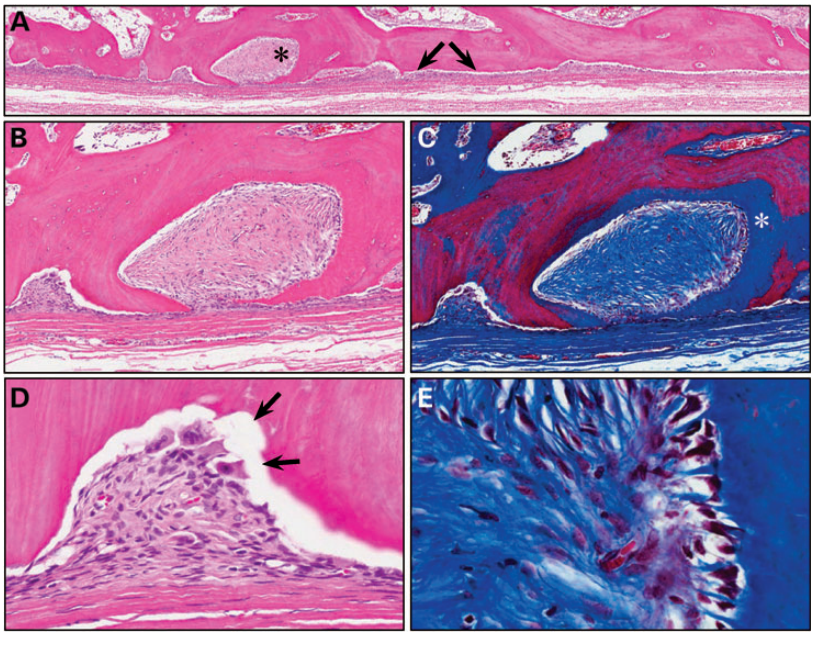

Figure 3. Dysplastic skeletal lesions from the rib of CSHS104. (**A**) Low power ($\times 2$) view from the pleural of the side of the rib shows a thin layer of cells that underlie the periostium along the length of the section of rib depicted (arrows). Asterisk denotes focus of dysplastic cells. (**B**) Higher power ($\times 4$) H&E of the area of dysplastic tissue marked by the asterisk in section (A) is shown. The lesion consists of a collection of fibroblast-like spindle-shaped cells in a relatively dense collagen matrix that appears to arise from the layer of dysplastic cells demonstrated in (A). (**C**) A Masson's trichrome stain of the same region seen in (B) displays both blue-staining collagen in the matrix surrounding the dysplastic fibroblast-like cells and an extensive area of osteoid surrounding the collection of dysplastic cells (asterisk). (**D**) A higher power ($\times 10$) view of the smaller area dysplastic cells seen in (B and C) show a collection of cells similarly arising from the layer of dysplastic cells seen in (A) as well as active osteoclast resorption of adjacent lamellar bone (arrows), suggesting that the dysplastic cells of CSHS can induce osteoclastogenesis. (**E**) A high power ($\times 40$) view of the region seen in (C) demonstrates collagen bundles connecting the osteoid with the pericellular matrix. The collagen bundles are parallel to the mineralizing surface (Sharpey's fibers) and interdigitate between the atypical but osteoblast-like cells that appear to have produced the adjacent osteoid.

Table 2. Somatic mutations in HRAS and NRAS identified by exome sequencing

Sample	Gene	Base change	Protein change	No. of reads in tissue		No. of reads in blood		*P*-value
				Ref.	Non-ref.	Ref.	Non-ref.	
CSHS101	*NRAS*	A>G	Q61R	097	033	129	0	1.3×10^{-11}
CSHS102	*HRAS*	G>C	G13R	188	093	159	0	9.0×10^{-22}
CSHS103	*HRAS*	A>G	Q61R	119	054	034	0	1.2×10^{-5}
CSHS104	*NRAS*	A>G	Q61R	235	152	NA	NA	NA
CSHS105	*HRAS*	G>C	G13R	029	015	069	0	1.3×10^{-6}

The *P*-values denoting the significance of the differences in reference (ref.) and non-references (non-ref.) reads in tissue versus blood were calculated using a one-tailed Fisher's exact test. In all cases, the respective *RAS* mutation carried the lowest *P*-value among all SNVs, and was the only variant with a quality score of ≥ 50 and a *P*-value of $< 1.0 \times 10^{-3}$. After correction for multiple testing, a value of 1.7×10^{-6} is considered the threshold for genome-wide significance. Given the biopsy technique, which samples both normal and affected tissue, admixture accounts for reduced mutant allele fraction in some samples.

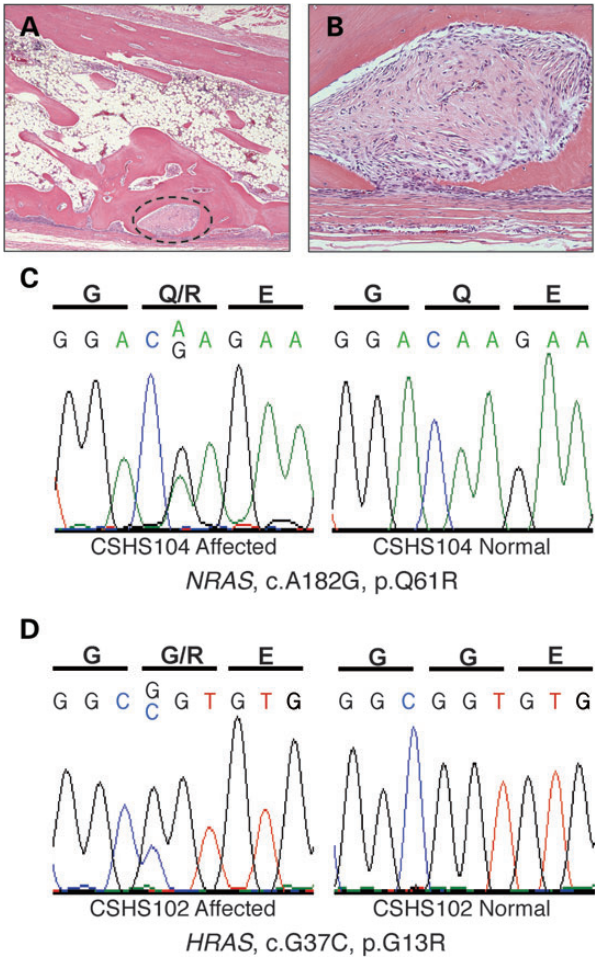

Figure 4. *NRAS* Q61R is present in dysplastic, but not normal, bone in CSHS102 and 104. (**A**) The region within the dotted line on a ×2 view of an affected rib from patient CSHS104 shows a representative region of dysplasia. DNA was extracted from cores of tissue excised from this region. (**B**) A ×20 view of the same region shown in (A) demonstrates an area of fibrous tissue composed of spindle-shaped cells set in a dense collagen matrix and in intimate association with the adjacent lamellar bone. (**C**) Sanger sequencing of DNA from affected bone tissue from patient CSHS104 shows the same heterozygous *NRAS* Q61R mutation that was found in the patient's cutaneous lesion (left panel). Sequence of DNA extracted from the patient CSHS104′s unaffected rib is wild type (right panel). (**D**) Sanger sequencing of DNA from a bone sample appearing grossly sclerotic from patient CSHS102 shows the heterozygous *HRAS* G13R mutation that was found in the patient's nevus (left panel). DNA from a region near the cortical bone is wild type (right panel).

immunohistochemistry (110). This suggests similarity between CSHS and oncogenic osteomalacia (a.k.a.TIO), a disorder in which primarily mesenchymal tumors secrete sufficient amounts of FGF23 to cause hypophosphatemia (41). These reports implicate Ras proteins in the regulation of FGF23, and our findings in CSHS provide the first evidence, suggesting that activating *RAS* mutations in bone cause elevated FGF23, hypophosphatemia, focal skeletal dysplasia and osteomalacia.

MATERIALS AND METHODS

Human subjects

All subjects provided written consent to the study protocol, which was approved by the Yale Human Investigation Committee. Each subject provided punch biopsies of affected skin as well as a blood sample. For one deceased case, archival tissue was obtained. One biopsy was used for direct DNA preparation in parallel with blood, and the other embedded for subsequent frozen sectioning.

DNA isolation

Genomic DNA from EN was obtained from fresh skin biopsies or 1 mm cores of formalin-fixed paraffin-embedded (FFPE) specimens, using DNeasy Micro (Qiagen, Valencia, CA, USA) with added deparaffinization performed for FFPE tissue. Fresh bone samples were powderized in liquid nitrogen and digest overnight in 10% (w/v) extraction buffer (EDTA 0.5 M, 1% *n*-lauroyl sarcosinate) and 10% (w/v) proteinase K (Qiagen, Valencia, CA, USA), and DNA was extracted using a standard phenol–chloroform protocols. FFPE samples were deparaffinized before proceeding as done for fresh bone. Blood DNA was also isolated via a standard phenol–chloroform protocol.

Whole-exome sequencing

Bar-coded libraries of sheared DNA isolated from tissue and blood were prepared, and whole-exome capture was performed (EZ Exome 2.0, Roche, Nutley, NJ, USA) by the Yale Center for Genome Analysis. Illumina HiSeq 2000 and 2500 instruments were used for sequencing blood samples pooled 6 per lane and tissue samples pooled 4 per lane with 75 bp paired end reads. Resulting reads were aligned to hg19 human reference using Efficient Large-scale Alignment of Nucleotide Databases

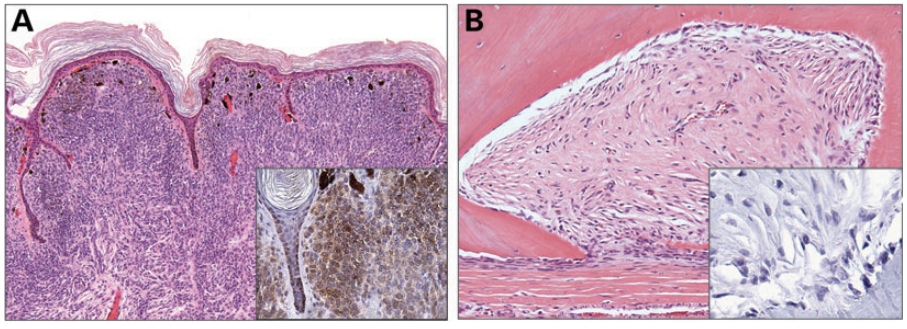

Figure 5. Affected skin, but not affected bone, shows staining for MelanA. Skin (**A**) and bone (**B**) specimens from patient CSHS104 confirmed to carry the *NRAS* Q61R mutation were sectioned and immunostained with melanocyte marker MelanA, to confirm the affected bone to be osteogenic and independent. Nuclei of abundant dermal melanocytes within a congenital nevus stain strongly brown for MelanA (A: ×10, ×20 insert), while a cellular region of dysplastic bone shows no staining (B: ×10, ×20 insert). A hematoxylin counterstain highlights nuclei in both panels.

software (ELAND, Illumina). Aligned reads were subsequently processed via a Perl script, which trimmed sequence to the targeted intervals and removed PCR duplicates. Single nucleotide variants (SNVs), deletions and insertions were identified using SAMtools software (111), and all variants were annotated for functional impact using a Perl script (112). We filtered our data to examine tissue variants with ≥2 non-reference reads in tissue and ≤4 non-reference reads in blood. The resulting data was filtered in Excel to exclude variants in 1000 Genomes (release 05/2011) and the National Heart, Lung and Blood Institute exome database (release ESP6500) from further analysis. Tissue variants in each sample were then filtered to examine coding mutations (missense, nonsense, splice site SNVs and insertions and deletions) with SAMtools quality scores ≥50 and coverage ≥8 and which were not present in 2577 control exomes. We then employed a one-tailed Fisher's exact test to compare mutant and wild-type read numbers in tissue and blood (genome-wide threshold for significance $\sim 1.7 \times 10^{-6}$, after Bonferroni correction for multiple testing of ∼30 000 genes). Aligned reads were examined with the Broad Institute Integrative Genomics Viewer (IGV) (113) to exclude variants resulting from alignment error.

Analysis of exome data for LOH

Exome CNV was employed to identify LOH segments of ≥1 Mbp with a *P*-value of ≤0.015 (114). LOH data were plotted by dividing the number of B-allele (non-reference) reads by the total number of reads independently for both tissue and blood at each SNV position. The difference in B-allele frequency values between tissue and blood was plotted against the genomic location.

Sanger sequencing

Verification of *RAS* mutations identified by exome sequencing was performed via standard PCR using Kapa 2G Fast polymerase (Kapa Biosystems, Woburn, MA, USA) and Sanger sequencing. The primers used are as follows:

HRAS Exon 2F: AGGTGGGGCAGGAGACCCTGTAG
HRAS Exon 2R: AGCCCTATCCTGGCTGTGTCCTG
HRAS Exon 3F: AGAGGCTGGCTGTGTGAACTCCC
HRAS Exon 3R: ACATGCGCAGAGAGGACAGGAGG
NRAS Exon 3F: GGGACAAACCAGATAGGCAGAAATGG
NRAS Exon 3R: TGGTAACCTCATTTCCCCATAAAGATTC

Immunohistochemistry

In order to exclude that the focus of dysplastic bone was the result of melanocytic metastasis and to confirm its osteogenic origin, the bone lesion was stained for melanocytic marker MelanA. Five-micrometer sections from FFPE tissue were deparaffinized using a xylene–ethanol gradient, rehydrated and rinsed in phosphate-buffered saline (PBS). Heat-induced antigen retrieval was performed by immersion in a modified pH 6.0 citrate buffer at 95°C for 30 min (Dako, Carpenteria, CA, USA). Slides were cooled, rinsed in PBS and endogenous peroxidase activity blocked by incubation in 3% H_2O_2 for 10 min, followed by washing, blocking in 10% normal goat serum and incubation with a 1:50 dilution of anti-MelanA primary antibody (IR633, Dako, Carpenteria, CA, USA). Slides were washed in PBS and incubated with an anti-mouse HRP secondary antibody for 1 h prior to substrate detection with 3,3′-diaminobenzidine tetrahydrochloride employed as a chromagen (LSAB+, Dako, Carpenteria, CA, USA). Hematoxylin with 1% ammonium hydroxide posttreatment was employed as a counterstain.

Investigation of the skin as potential source of FGF23 was done via staining affected skin tissue with FGF23 antibody (Immunotopics, San Clemente, CA, USA). Six-micrometer sections of frozen or FFPE lesional skin tissue were either fixed using a 1:1 mixture of acetone and methanol and rinsed in PBS or deparaffinized using a xylene-ethanol gradient, rehydrated and rinsed in PBS, respectively. For FFPE sections, heat-induced antigen retrieval was performed as previously described. Slides were cooled, rinsed and blocked in 10% normal donkey serum and 1% bovine serum albumin, prior to incubation for 2 h at room temperature with a 1:100 dilution of anti-FGF23 primary antibody (IR633, Dako, Carpenteria, CA, USA). Slides were washed in PBS and incubated with an anti-goat Cy3 fluorescent secondary antibody for 1 h at room temperature, and washed again. Slides were incubated with 1× DAPI diluted in PBS for 3 min and mounted using Mowiol.

SUPPLEMENTARY MATERIAL

Supplementary Material is available at *HMG* online.

ACKNOWLEDGEMENTS

We thank Lynn Boyden for critical review of the manuscript, and Jing Zhou, Li Tian, Britt Craiglow, Carol Nelson-Williams, Gerald Goh, Vincent Klump and Brian Zhao for technical assistance. We also thank Thomas Carpenter, Veraragavan Eswarakumar and Karl Insogna for insightful correspondence on endocrinology and bone biology.

Conflict of Interest statement. None declared.

FUNDING

This work was supported by a Doris Duke Charitable Foundation Clinical Scientist Development Award to K.A.C. and by the Yale Center for Mendelian Genomics (NIH U54 HG006504). Y.H.L. was supported by the Paul H. Lavietes, M.D. Student Research Fellowship from the Yale University School of Medicine. D.O. was supported by the "la Caixa" Fellowship Program. M.T.C. and R.I.G. were supported by the Division of Intramural Research, National Institutes of Dental and Craniofacial Research, NIH.

REFERENCES

1. Blaschko, A. (1901) Die Nervenverteilung in der Haut in ihrer Beziehung zu den Erkrankungen der Haut. *Beilage zu den Verhandlungen der Deutschen Dermatologischen Gesellschaft VII Congress. Breslau, Braumuller, Wien, 1901*.
2. Happle, R. (1986) The McCune-Albright syndrome: a lethal gene surviving by mosaicism. *Clin. Genet.*, **29**, 321–324.
3. Rieger, E., Kofler, R., Borkenstein, M., Schwingshandl, J., Soyer, H.P. and Kerl, H. (1994) Melanotic macules following Blaschko's lines in McCune-Albright syndrome. *Br. J. Dermatol.*, **130**, 215–220.
4. Tannous, Z.S., Mihm, M.C. Jr., Sober, A.J. and Duncan, L.M. (2005) Congenital melanocytic nevi: clinical and histopathologic features, risk of melanoma, and clinical management. *J. Am. Acad. Dermatol.*, **52**, 197–203.
5. Vujevich, J.J. and Mancini, A.J. (2004) The epidermal nevus syndromes: multisystem disorders. *J. Am. Acad. Dermatol.*, **50**, 957–961.
6. Amato, C., Elia, M. and Schepis, C. (2010) Schimmelpenning syndrome: a kind of craniofacial epidermal nevus associated with cerebral and ocular MR imaging abnormalities. *AJNR Am. J. Neuroradiol.*, **31**, E47–48.
7. Lee, W.J., Lee, S.M., Won, C.H., Chang, S.E., Lee, M.W., Choi, J.H. and Moon, K.C. (2013) Coexistence of congenital giant melanocytic nevus of the scalp with cranial defect, poliosis, and hair loss. *Pediatr. Dermatol.*, doi: 10.1111/pde.12101.
8. Sharma, R., Singal, A., Verma, P., Rohatgi, J. and Sharma, S. (2012) Epidermal nevus syndrome associated with unusual neurological, ocular, and skeletal features. *Indian J. Dermatol. Venereol. Leprol.*, **78**, 480–483.
9. Xu, H., Cerrato, F. and Baldini, A. (2005) Timed mutation and cell-fate mapping reveal reiterated roles of Tbx1 during embryogenesis, and a crucial function during segmentation of the pharyngeal system via regulation of endoderm expansion. *Development*, **132**, 4387–4395.
10. Zhou, W., Tan, Y., Anderson, D.J., Crist, E.M., Ruohola-Baker, H., Salipante, S.J. and Horwitz, M.S. (2013) Use of somatic mutations to quantify random contributions to mouse development. *BMC Genomics*, **14**, 39.
11. Braun-Falco, O. (2000) *Dermatology*. Springer, Berlin, New York.
12. Heddle, J.A. (1999) On clonal expansion and its effects on mutant frequencies, mutation spectra and statistics for somatic mutations in vivo. *Mutagenesis*, **14**, 257–260.
13. Kaliyadan, F., Nampoothiri, S., Sunitha, V. and Kuruvilla, V.E. (2010) Nevus comedonicus syndrome–nevus comedonicus associated with ipsilateral polysyndactyly and bilateral oligodontia. *Pediatr. Dermatol.*, **27**, 377–379.
14. Sugarman, G.I. and Reed, W.B. (1969) Two unusual neurocutaneous disorders with facial cutaneous signs. *Arch. Neurol.*, **21**, 242–247.
15. Alsohim, F., Abou-Jaoude, P., Ninet, J., Pracros, J.P., Phan, A. and Cochat, P. (2011) Bilateral renal artery stenosis and epidermal nevus syndrome in a child. *Pediatr. Nephrol.*, **26**, 2081–2084.
16. Feuerstein, R.C. and Mims, L.C. (1962) Linear nevus sebaceus with convulsions and mental retardation. *Am. J. Dis. Child.*, **104**, 675–679.
17. Schimmelpenning, G.W. (1957) [Clinical contribution to symptomatology of phacomatosis]. *Fortschr. Geb. Rontgenstr. Nuklearmed.*, **87**, 716–720.
18. Becker, S.W. (1949) Concurrent melanosis and hypertrichosis in distribution of nevus unius lateris. *Arch. Derm. Syphilol.*, **60**, 155–160.
19. Aschinberg, L.C., Solomon, L.M., Zeis, P.M., Justice, P. and Rosenthal, I.M. (1977) Vitamin D-resistant rickets associated with epidermal nevus syndrome: demonstration of a phosphaturic substance in the dermal lesions. *J. Pediatr.*, **91**, 56–60.
20. Carey, D.E., Drezner, M.K., Hamdan, J.A., Mange, M., Ahmad, M.S., Mubarak, S. and Nyhan, W.L. (1986) Hypophosphatemic rickets/osteomalacia in linear sebaceous nevus syndrome: a variant of tumor-induced osteomalacia. *J. Pediatr.*, **109**, 994–1000.
21. Chou, Y.Y., Chao, S.C., Shiue, C.N., Tsai, W.H. and Lin, S.J. (2005) Hypophosphatemic rickets associated with epidermal nevus syndrome and giant hairy nevus. *J. Pediatr. Endocrinol. Metab.*, **18**, 93–95.
22. Chou, Y.Y., Chao, S.C., Tsai, S.C. and Lin, S.J. (2005) Novel PHEX gene mutations in two Taiwanese patients with hypophosphatemic rickets. *J. Formos. Med. Assoc.*, **104**, 198–202.
23. Gathwala, G., Dalal, P., Dalal, J.S., Dayal, S. and Singh, G. (2013) Giant congenital melanocytic nevi: a rare association with hypophosphatemic rickets. *Indian J. Pediatr.*, **80**, 430–431.
24. Goldblum, J.R. and Headington, J.T. (1993) Hypophosphatemic vitamin D-resistant rickets and multiple spindle and epithelioid nevi associated with linear nevus sebaceus syndrome. *J. Am. Acad. Dermatol.*, **29**, 109–111.
25. Heike, C.L., Cunningham, M.L., Steiner, R.D., Wenkert, D., Hornung, R.L., Gruss, J.S., Gannon, F.H., McAlister, W.H., Mumm, S. and Whyte, M.P. (2005) Skeletal changes in epidermal nevus syndrome: does focal bone disease harbor clues concerning pathogenesis? *Am. J. Med. Genet. A*, **139A**, 67–77.
26. Hoffman, W.H., Jueppner, H.W., Deyoung, B.R., O'Dorisio, MS. and Given, K.S. (2005) Elevated fibroblast growth factor-23 in hypophosphatemic linear nevus sebaceous syndrome. *Am. J. Med. Genet. A*, **134**, 233–236.
27. Hosalkar, H.S., Jones, D.H., Offiah, A. and Hall, C. (2003) Linear sebaceous naevus syndrome and resistant rickets. *J. Bone Joint Surg. Br.*, **85**, 578–583.
28. Ivker, R., Resnick, S.D. and Skidmore, R.A. (1997) Hypophosphatemic vitamin D-resistant rickets, precocious puberty, and the epidermal nevus syndrome. *Arch. Dermatol.*, **133**, 1557–1561.
29. Kishida, E.S., Muniz Silva, M.A., da Costa Pereira, F., Sanches, J.A. Jr. and Sotto, M.N. (2005) Epidermal nevus syndrome associated with adnexal tumors, spitz nevus, and hypophosphatemic vitamin D-resistant rickets. *Pediatr. Dermatol.*, **22**, 48–54.
30. Moorjani, R. and Shaw, D.G. (1976) Feuerstein and Mims syndrome with resistant rickets. *Pediatr. Radiol.*, **5**, 120–122.
31. Moreira, A.I., Ferreira, G., Santos, M., Baptista, A. and Ferreira, E.O. (2010) Epidermal nevus syndrome associated with hypophosphatemic rickets. *Dermatol. Online J.*, **16**, 14.
32. Narazaki, R., Ihara, K., Namba, N., Matsuzaki, H., Ozono, K. and Hara, T. (2012) Linear nevus sebaceous syndrome with hypophosphatemic rickets with elevated FGF-23. *Pediatr. Nephrol.*, **27**, 861–863.
33. Olivares, J.L., Ramos, F.J., Carapeto, F.J. and Bueno, M. (1999) Epidermal naevus syndrome and hypophosphataemic rickets: description of a patient with central nervous system anomalies and review of the literature. *Eur. J. Pediatr.*, **158**, 103–107.
34. Oranje, A.P., Przyrembel, H., Meradji, M., Loonen, M.C. and de Klerk, J.B. (1994) Solomon's epidermal nevus syndrome (type: linear nevus sebaceus) and hypophosphatemic vitamin D-resistant rickets. *Arch. Dermatol.*, **130**, 1167–1171.
35. Sethi, S.K., Hari, P. and Bagga, A. (2010) Elevated FGF-23 and parathormone in linear nevus sebaceous syndrome with resistant rickets. *Pediatr. Nephrol.*, **25**, 1577–1578.
36. Skovby, F., Svejgaard, E. and Moller, J. (1987) Hypophosphatemic rickets in linear sebaceous nevus sequence. *J. Pediatr.*, **111**, 855–857.

37. Tokatli, A., Coskun, T. and Ozalp, I. (1997) Hypophosphatemic vitamin-D resistant rickets associated with epidermal nevus syndrome. A case report. *Turk. J. Pediatr.*, **39**, 247–251.
38. O'Neill, E.M. (1993) Linear sebaceous naevus syndrome with oncogenic rickets and diffuse pulmonary angiomatosis. *J. R. Soc. Med.*, **86**, 177–178.
39. Stosiek, N., Hornstein, O.P., Hiller, D. and Peters, K.P. (1994) Extensive linear epidermal nevus associated with hemangiomas of bones and vitamin-D-resistant rickets. *Dermatology*, **189**, 278–282.
40. Perwad, F., Zhang, M.Y., Tenenhouse, H.S. and Portale, A.A. (2007) Fibroblast growth factor 23 impairs phosphorus and vitamin D metabolism in vivo and suppresses 25-hydroxyvitamin D-1alpha-hydroxylase expression in vitro. *Am. J. Physiol. Renal Physiol.*, **293**, F1577–1583.
41. Shimada, T., Mizutani, S., Muto, T., Yoneya, T., Hino, R., Takeda, S., Takeuchi, Y., Fujita, T., Fukumoto, S. and Yamashita, T. (2001) Cloning and characterization of FGF23 as a causative factor of tumor-induced osteomalacia. *Proc. Natl Acad. Sci. USA*, **98**, 6500–6505.
42. Shimada, T., Urakawa, I., Yamazaki, Y., Hasegawa, H., Hino, R., Yoneya, T., Takeuchi, Y., Fujita, T., Fukumoto, S. and Yamashita, T. (2004) FGF-23 transgenic mice demonstrate hypophosphatemic rickets with reduced expression of sodium phosphate cotransporter type IIa. *Biochem. Biophys. Res. Commun.*, **314**, 409–414.
43. Hafner, C., Toll, A. and Real, F.X. (2011) HRAS mutation mosaicism causing urothelial cancer and epidermal nevus. *N. Engl. J. Med.*, **365**, 1940–1942.
44. Kinsler, V.A., Thomas, A.C., Ishida, M., Bulstrode, N.W., Loughlin, S., Hing, S., Chalker, J., McKenzie, K., Abu-Amero, S., Slater, O. *et al.* (2013) Multiple congenital melanocytic nevi and neurocutaneous melanosis are caused by postzygotic mutations in codon 61 of NRAS. *J. Invest. Dermatol.*, **133**, 2236–2296.
45. Levinsohn, J.L., Tian, L.C., Boyden, L.M., McNiff, J.M., Narayan, D., Loring, E.S., Yun, D., Sugarman, J.L., Overton, J.D., Mane, S.M. *et al.* (2013) Whole-exome sequencing reveals somatic mutations in HRAS and KRAS, which cause nevus sebaceus. *J. Invest. Dermatol.*, **133**, 827–830.
46. Hafner, C., Toll, A., Gantner, S., Mauerer, A., Lurkin, I., Acquadro, F., Fernandez-Casado, A., Zwarthoff, E.C., Dietmaier, W., Baselga, E. *et al.* (2012) Keratinocytic epidermal nevi are associated with mosaic RAS mutations. *J. Med. Genet.*, **49**, 249–253.
47. Groesser, L., Herschberger, E., Ruetten, A., Ruivenkamp, C., Lopriore, E., Zutt, M., Langmann, T., Singer, S., Klingseisen, L., Schneider-Brachert, W. *et al.* (2012) Postzygotic HRAS and KRAS mutations cause nevus sebaceous and Schimmelpenning syndrome. *Nat. Genet.*, **44**, 783–787.
48. Lorenz-Depiereux, B., Bastepe, M., Benet-Pages, A., Amyere, M., Wagenstaller, J., Muller-Barth, U., Badenhoop, K., Kaiser, S.M., Rittmaster, R.S., Shlossberg, A.H. *et al.* (2006) DMP1 mutations in autosomal recessive hypophosphatemia implicate a bone matrix protein in the regulation of phosphate homeostasis. *Nat. Genet.*, **38**, 1248–1250.
49. Saito, T., Nishii, Y., Yasuda, T., Ito, N., Suzuki, H., Igarashi, T., Fukumoto, S. and Fujita, T. (2009) Familial hypophosphatemic rickets caused by a large deletion in PHEX gene. *Eur. J. Endocrinol.*, **161**, 647–651.
50. Saito, T., Shimizu, Y., Hori, M., Taguchi, M., Igarashi, T., Fukumoto, S. and Fujitab, T. (2011) A patient with hypophosphatemic rickets and ossification of posterior longitudinal ligament caused by a novel homozygous mutation in ENPP1 gene. *Bone*, **49**, 913–916.
51. White, K.E., Carn, G., Lorenz-Depiereux, B., Benet-Pages, A., Strom, T.M. and Econs, M.J. (2001) Autosomal-dominant hypophosphatemic rickets (ADHR) mutations stabilize FGF-23. *Kidney Int.*, **60**, 2079–2086.
52. Brownstein, C.A., Adler, F., Nelson-Williams, C., Iijima, J., Li, P., Imura, A., Nabeshima, Y., Reyes-Mugica, M., Carpenter, T.O. and Lifton, R.P. (2008) A translocation causing increased alpha-klotho level results in hypophosphatemic rickets and hyperparathyroidism. *Proc. Natl Acad. Sci. USA*, **105**, 3455–3460.
53. White, K.E., Cabral, J.M., Davis, S.I., Fishburn, T., Evans, W.E., Ichikawa, S., Fields, J., Yu, X., Shaw, N.J., McLellan, N.J. *et al.* (2005) Mutations that cause osteoglophonic dysplasia define novel roles for FGFR1 in bone elongation. *Am. J. Hum. Genet.*, **76**, 361–367.
54. Saraswat, A., Dogra, S., Bansali, A. and Kumar, B. (2003) Phakomatosis pigmentokeratotica associated with hypophosphataemic vitamin D-resistant rickets: improvement in phosphate homeostasis after partial laser ablation. *Br. J. Dermatol.*, **148**, 1074–1076.
55. Reddy, E.P., Reynolds, R.K., Santos, E. and Barbacid, M. (1982) A point mutation is responsible for the acquisition of transforming properties by the T24 human bladder carcinoma oncogene. *Nature*, **300**, 149–152.
56. Tabin, C.J., Bradley, S.M., Bargmann, C.I., Weinberg, R.A., Papageorge, A.G., Scolnick, E.M., Dhar, R., Lowy, D.R. and Chang, E.H. (1982) Mechanism of activation of a human oncogene. *Nature*, **300**, 143–149.
57. Taparowsky, E., Suard, Y., Fasano, O., Shimizu, K., Goldfarb, M. and Wigler, M. (1982) Activation of the T24 bladder carcinoma transforming gene is linked to a single amino acid change. *Nature*, **300**, 762–765.
58. Taparowsky, E., Shimizu, K., Goldfarb, M. and Wigler, M. (1983) Structure and activation of the human N-ras gene. *Cell*, **34**, 581–586.
59. Yuasa, Y., Srivastava, S.K., Dunn, C.Y., Rhim, J.S., Reddy, E.P. and Aaronson, S.A. (1983) Acquisition of transforming properties by alternative point mutations within c-bas/has human proto-oncogene. *Nature*, **303**, 775–779.
60. Brown, R., Marshall, C.J., Pennie, S.G. and Hall, A. (1984) Mechanism of activation of an N-ras gene in the human fibrosarcoma cell line HT1080. *EMBO J.*, **3**, 1321–1326.
61. Bos, J.L., Toksoz, D., Marshall, C.J., Verlaan-de Vries, M., Veeneman, G.H., van der Eb, A.J., van Boom, J.H., Janssen, J.W. and Steenvoorden, A.C. (1985) Amino-acid substitutions at codon 13 of the N-ras oncogene in human acute myeloid leukaemia. *Nature*, **315**, 726–730.
62. Wiseman, R.W., Stowers, S.J., Miller, E.C., Anderson, M.W. and Miller, J.A. (1986) Activating mutations of the c-Ha-ras protooncogene in chemically induced hepatomas of the male B6C3 F1 mouse. *Proc. Natl Acad. Sci. USA*, **83**, 5825–5829.
63. Barbacid, M. (1987) ras genes. *Annu. Rev. Biochem.*, **56**, 779–827.
64. Xu, C., Rosler, E., Jiang, J., Lebkowski, J.S., Gold, J.D., O'Sullivan, C., Delavan-Boorsma, K., Mok, M., Bronstein, A. and Carpenter, M.K. (2005) Basic fibroblast growth factor supports undifferentiated human embryonic stem cell growth without conditioned medium. *Stem Cells*, **23**, 315–323.
65. Xiao, L., Naganawa, T., Lorenzo, J., Carpenter, T.O., Coffin, J.D. and Hurley, M.M. (2010) Nuclear isoforms of fibroblast growth factor 2 are novel inducers of hypophosphatemia via modulation of FGF23 and KLOTHO. *J. Biol. Chem.*, **285**, 2834–2846.
66. Wang, X., Wang, S., Li, C., Gao, T., Liu, Y., Rangiani, A., Sun, Y., Hao, J., George, A., Lu, Y. *et al.* (2012) Inactivation of a novel FGF23 regulator, FAM20C, leads to hypophosphatemic rickets in mice. *PLoS Genet.*, **8**, e1002708.
67. Topaz, O., Shurman, D.L., Bergman, R., Indelman, M., Ratajczak, P., Mizrachi, M., Khamaysi, Z., Behar, D., Petronius, D., Friedman, V. *et al.* (2004) Mutations in GALNT3, encoding a protein involved in O-linked glycosylation, cause familial tumoral calcinosis. *Nat. Genet.*, **36**, 579–581.
68. Sun, Y., Prasad, M., Gao, T., Wang, X., Zhu, Q., D'Souza, R., Feng, J.Q. and Qin, C. (2010) Failure to process dentin matrix protein 1 (DMP1) into fragments leads to its loss of function in osteogenesis. *J. Biol. Chem.*, **285**, 31713–31722.
69. Segawa, H., Onitsuka, A., Furutani, J., Kaneko, I., Aranami, F., Matsumoto, N., Tomoe, Y., Kuwahata, M., Ito, M., Matsumoto, M. *et al.* (2009) Npt2a and Npt2c in mice play distinct and synergistic roles in inorganic phosphate metabolism and skeletal development. *Am. J. Physiol. Renal Physiol.*, **297**, F671–678.
70. Rowe, P.S., Oudet, C.L., Francis, F., Sinding, C., Pannetier, S., Econs, M.J., Strom, T.M., Meitinger, T., Garabedian, M., David, A. *et al.* (1997) Distribution of mutations in the PEX gene in families with X-linked hypophosphataemic rickets (HYP). *Hum. Mol. Genet.*, **6**, 539–549.
71. Rowe, P.S., de Zoysa, P.A., Dong, R., Wang, H.R., White, K.E., Econs, M.J. and Oudet, C.L. (2000) MEPE, a new gene expressed in bone marrow and tumors causing osteomalacia. *Genomics*, **67**, 54–68.
72. Rafaelsen, S.H., Raeder, H., Fagerheim, A.K., Knappskog, P., Carpenter, T.O., Johansson, S. and Bjerknes, R. (2013) Exome sequencing reveals FAM20c mutations associated with fibroblast growth factor 23-related hypophosphatemia, dental anomalies, and ectopic calcification. *J. Bone Miner. Res.*, **28**, 1378–1385.
73. Quarles, L.D. (2003) FGF23, PHEX, and MEPE regulation of phosphate homeostasis and skeletal mineralization. *Am. J. Physiol. Endocrinol. Metab.*, **285**, E1–9.
74. Olauson, H., Krajisnik, T., Larsson, C., Lindberg, B. and Larsson, T.E. (2008) A novel missense mutation in GALNT3 causing hyperostosis-hyperphosphataemia syndrome. *Eur. J. Endocrinol.*, **158**, 929–934.
75. Narisawa, S., Yadav, M.C. and Millan, J.L. (2013) In vivo overexpression of tissue-nonspecific alkaline phosphatase increases skeletal mineralization and affects the phosphorylation status of osteopontin. *J. Bone Miner. Res.*, **28**, 1587–1598.
76. Lorenz-Depiereux, B., Schnabel, D., Tiosano, D., Hausler, G. and Strom, T.M. (2010) Loss-of-function ENPP1 mutations cause both generalized

arterial calcification of infancy and autosomal-recessive hypophosphatemic rickets. *Am. J. Hum. Genet.*, **86**, 267–272.
77. Lorenz-Depiereux, B., Benet-Pages, A., Eckstein, G., Tenenbaum-Rakover, Y., Wagenstaller, J., Tiosano, D., Gershoni-Baruch, R., Albers, N., Lichtner, P., Schnabel, D. *et al.* (2006) Hereditary hypophosphatemic rickets with hypercalciuria is caused by mutations in the sodium-phosphate cotransporter gene SLC34A3. *Am. J. Hum. Genet.*, **78**, 193–201.
78. Liu, S., Guo, R., Simpson, L.G., Xiao, Z.S., Burnham, C.E. and Quarles, L.D. (2003) Regulation of fibroblastic growth factor 23 expression but not degradation by PHEX. *J. Biol. Chem.*, **278**, 37419–37426.
79. Levy-Litan, V., Hershkovitz, E., Avizov, L., Leventhal, N., Bercovich, D., Chalifa-Caspi, V., Manor, E., Buriakovsky, S., Hadad, Y., Goding, J. *et al.* (2010) Autosomal-recessive hypophosphatemic rickets is associated with an inactivation mutation in the ENPP1 gene. *Am. J. Hum. Genet.*, **86**, 273–278.
80. Kurosu, H., Ogawa, Y., Miyoshi, M., Yamamoto, M., Nandi, A., Rosenblatt, K.P., Baum, M.G., Schiavi, S., Hu, M.C., Moe, O.W. *et al.* (2006) Regulation of fibroblast growth factor-23 signaling by klotho. *J. Biol. Chem.*, **281**, 6120–6123.
81. Kelleher, C.L., Buckalew, V.M., Frederickson, E.D., Rhodes, D.J., Conner, D.A., Seidman, J.G. and Seidman, C.E. (1998) CLCN5 mutation Ser244Leu is associated with X-linked renal failure without X-linked recessive hypophosphatemic rickets. *Kidney Int.*, **53**, 31–37.
82. Iwaki, T., Sandoval-Cooper, M.J., Tenenhouse, H.S. and Castellino, F.J. (2008) A missense mutation in the sodium phosphate co-transporter Slc34a1 impairs phosphate homeostasis. *J. Am. Soc. Nephrol.*, **19**, 1753–1762.
83. Hughes, M.R., Malloy, P.J., Kieback, D.G., Kesterson, R.A., Pike, J.W., Feldman, D. and O'Malley, B.W. (1988) Point mutations in the human vitamin D receptor gene associated with hypocalcemic rickets. *Science*, **242**, 1702–1705.
84. Holm, I.A., Huang, X. and Kunkel, L.M. (1997) Mutational analysis of the PEX gene in patients with X-linked hypophosphatemic rickets. *Am. J. Hum. Genet.*, **60**, 790–797.
85. Harmey, D., Johnson, K.A., Zelken, J., Camacho, N.P., Hoylaerts, M.F., Noda, M., Terkeltaub, R. and Millan, J.L. (2006) Elevated skeletal osteopontin levels contribute to the hypophosphatasia phenotype in Akp2(-/-) mice. *J. Bone Miner. Res.*, **21**, 1377–1386.
86. Gattineni, J., Bates, C., Twombley, K., Dwarakanath, V., Robinson, M.L., Goetz, R., Mohammadi, M. and Baum, M. (2009) FGF23 decreases renal NaPi-2a and NaPi-2c expression and induces hypophosphatemia in vivo predominantly via FGF receptor 1. *Am. J. Physiol. Renal Physiol.*, **297**, F282–291.
87. Garringer, H.J., Malekpour, M., Esteghamat, F., Mortazavi, S.M., Davis, S.I., Farrow, E.G., Yu, X., Arking, D.E., Dietz, H.C. and White, K.E. (2008) Molecular genetic and biochemical analyses of FGF23 mutations in familial tumoral calcinosis. *Am. J. Physiol. Endocrinol. Metab.*, **295**, E929–937.
88. Frishberg, Y., Topaz, O., Bergman, R., Behar, D., Fisher, D., Gordon, D., Richard, G. and Sprecher, E. (2005) Identification of a recurrent mutation in GALNT3 demonstrates that hyperostosis-hyperphosphatemia syndrome and familial tumoral calcinosis are allelic disorders. *J. Mol. Med. (Berl.)*, **83**, 33–38.
89. Francis, F., Strom, T.M., Hennig, S., Boddrich, A., Lorenz, B., Brandau, O., Mohnike, K.L., Cagnoli, M., Steffens, C., Klages, S. *et al.* (1997) Genomic organization of the human PEX gene mutated in X-linked dominant hypophosphatemic rickets. *Genome Res.*, **7**, 573–585.
90. Fisher, S.E., Black, G.C., Lloyd, S.E., Hatchwell, E., Wrong, O., Thakker, R.V. and Craig, I.W. (1994) Isolation and partial characterization of a chloride channel gene which is expressed in kidney and is a candidate for Dent's disease (an X-linked hereditary nephrolithiasis). *Hum. Mol. Genet.*, **3**, 2053–2059.
91. Feng, J.Q., Ward, L.M., Liu, S., Lu, Y., Xie, Y., Yuan, B., Yu, X., Rauch, F., Davis, S.I., Zhang, S. *et al.* (2006) Loss of DMP1 causes rickets and osteomalacia and identifies a role for osteocytes in mineral metabolism. *Nat. Genet.*, **38**, 1310–1315.
92. Econs, M.J., Friedman, N.E., Rowe, P.S., Speer, M.C., Francis, F., Strom, T.M., Oudet, C., Smith, J.A., Ninomiya, J.T., Lee, B.E. *et al.* (1998) A PHEX gene mutation is responsible for adult-onset vitamin D-resistant hypophosphatemic osteomalacia: evidence that the disorder is not a distinct entity from X-linked hypophosphatemic rickets. *J. Clin. Endocrinol. Metab.*, **83**, 3459–3462.
93. Carpenter, T.O., Ellis, B.K., Insogna, K.L., Philbrick, W.M., Sterpka, J. and Shimkets, R. (2005) Fibroblast growth factor 7: an inhibitor of phosphate transport derived from oncogenic osteomalacia-causing tumors. *J. Clin. Endocrinol. Metab.*, **90**, 1012–1020.
94. Berndt, T., Craig, T.A., Bowe, A.E., Vassiliadis, J., Reczek, D., Finnegan, R., Jan De Beur, S.M., Schiavi, S.C. and Kumar, R. (2003) Secreted frizzled-related protein 4 is a potent tumor-derived phosphaturic agent. *J. Clin. Invest.*, **112**, 785–794.
95. Bai, X.Y., Miao, D., Goltzman, D. and Karaplis, A.C. (2003) The autosomal dominant hypophosphatemic rickets R176Q mutation in fibroblast growth factor 23 resists proteolytic cleavage and enhances in vivo biological potency. *J. Biol. Chem.*, **278**, 9843–9849.
96. White, K.E., Lorenz, B., Evans, W.E., Speer, M.C., O'Riordan, J.L.H., Meitinger, T., Strom, T.M. and Econs, M.J. (2000) Autosomal dominant hypophosphatemic rickets is caused by mutations in a novel gene, FGF21, that shares homology with the fibroblast growth factor family. *J. Bone Miner. Res.*, **15**, S153–S153.
97. White, K.E., Lorenz, B., Evans, W.E., Meitinger, T., Strom, T.M. and Econs, M.J. (2000) Molecular cloning of a novel human UDP-GalNAc : polypeptide N-acetylgalactosaminyltransferase, GalNAc-T8, and analysis as a candidate autosomal dominant hypophosphatemic rickets (ADHR) gene. *Gene*, **246**, 347–356.
98. White, K.E., Cabral, J.M., Evans, W.E., Ichikawa, S., Davis, S.I. and Econs, M.J. (2003) A missense mutation in FGFR1 causes a novel syndrome: Craniofacial dysplasia with hypophosphatemia (CFDH). *J. Bone Miner. Res.*, **18**, S4–S4.
99. Albright, F., Butler, A.M., Hampton, A.O. and Smith, P. (1937) Syndrome characterized by osteitis fibrosa disseminata, areas of pigmentation and endocrine dysfunction, with precocious puberty in females – report of five cases. *N. Engl. J. Med.*, **216**, 727–746.
100. Riminucci, M., Collins, M.T., Fedarko, N.S., Cherman, N., Corsi, A., White, K.E., Waguespack, S., Gupta, A., Hannon, T., Econs, M.J. *et al.* (2003) FGF-23 in fibrous dysplasia of bone and its relationship to renal phosphate wasting. *J. Clin. Invest.*, **112**, 683–692.
101. Kobayashi, K., Imanishi, Y., Koshiyama, H., Miyauchi, A., Wakasa, K., Kawata, T., Goto, H., Ohashi, H., Koyano, H.M., Mochizuki, R. *et al.* (2006) Expression of FGF23 is correlated with serum phosphate level in isolated fibrous dysplasia. *Life Sci.*, **78**, 2295–2301.
102. Weinstein, L.S., Shenker, A., Gejman, P.V., Merino, M.J., Friedman, E. and Spiegel, A.M. (1991) Activating mutations of the stimulatory G protein in the McCune-Albright syndrome. *N. Engl. J. Med.*, **325**, 1688–1695.
103. Bhattacharyya, N., Wiench, M., Dumitrescu, C., Connolly, B.M., Bugge, T.H., Patel, H.V., Gafni, R.I., Cherman, N., Cho, M., Hager, G.L. *et al.* (2012) Mechanism of FGF23 processing in fibrous dysplasia. *J. Bone Miner. Res.*, **27**, 1132–1141.
104. de Sanctis, L., Delmastro, L., Russo, M.C., Matarazzo, P., Lala, R. and de Sanctis, C. (2006) Genetics of McCune-Albright syndrome. *J. Pediatr. Endocrinol. Metab.*, **19**(Suppl. 2), 577–582.
105. Kim, I.S., Kim, E.R., Nam, H.J., Chin, M.O., Moon, Y.H., Oh, M.R., Yeo, U.C., Song, S.M., Kim, J.S., Uhm, M.R. *et al.* (1999) Activating mutation of GS alpha in McCune-Albright syndrome causes skin pigmentation by tyrosinase gene activation on affected melanocytes. *Horm. Res.*, **52**, 235–240.
106. Groesser, L., Herschberger, E., Sagrera, A., Shwayder, T., Flux, K., Ehmann, L., Wollenberg, A., Torrelo, A., Bagazgoitia, L., Diaz-Ley, B. *et al.* (2013) Phacomatosis pigmentokeratotica is caused by a postzygotic HRAS mutation in a multipotent progenitor cell. *J. Invest. Dermatol.*, **133**, 1998–2003.
107. Camalier, C.E., Young, M.R., Bobe, G., Perella, C.M., Colburn, N.H. and Beck, G.R. Jr. (2010) Elevated phosphate activates N-ras and promotes cell transformation and skin tumorigenesis. *Cancer Prev. Res. (Phila.)*, **3**, 359–370.
108. Antoniucci, D.M., Yamashita, T. and Portale, A.A. (2006) Dietary phosphorus regulates serum fibroblast growth factor-23 concentrations in healthy men. *J. Clin. Endocrinol. Metab.*, **91**, 3144–3149.
109. Conrads, K.A., Yi, M., Simpson, K.A., Lucas, D.A., Camalier, C.E., Yu, L.R., Veenstra, T.D., Stephens, R.M., Conrads, T.P. and Beck, G.R. Jr (2005) A combined proteome and microarray investigation of inorganic phosphate-induced pre-osteoblast cells. *Mol. Cell. Proteomics*, **4**, 1284–1296.
110. Leaf, D.E., Pereira, R.C., Bazari, H. and Juppner, H. (2013) Oncogenic osteomalacia due to FGF23-expressing colon adenocarcinoma. *J. Clin. Endocrinol. Metab.*, **98**, 887–891.

111. Li, H., Handsaker, B., Wysoker, A., Fennell, T., Ruan, J., Homer, N., Marth, G., Abecasis, G. and Durbin, R. (2009) The sequence alignment/map format and SAMtools. *Bioinformatics*, **25**, 2078–2079.
112. Choi, M., Scholl, U.I., Ji, W., Liu, T., Tikhonova, I.R., Zumbo, P., Nayir, A., Bakkaloglu, A., Ozen, S., Sanjad, S. *et al.* (2009) Genetic diagnosis by whole exome capture and massively parallel DNA sequencing. *Proc. Natl Acad. Sci. USA*, **106**, 19096–19101.
113. Thorvaldsdottir, H., Robinson, J.T. and Mesirov, J.P. (2012) Integrative genomics viewer (IGV): high-performance genomics data visualization and exploration. *Briefings in Bioinformatics*, **14**, 178–192.
114. Sathirapongsasuti, J.F., Lee, H., Horst, B.A., Brunner, G., Cochran, A.J., Binder, S., Quackenbush, J. and Nelson, S.F. (2011) Exome sequencing-based copy-number variation and loss of heterozygosity detection: ExomeCNV. *Bioinformatics*, **27**, 2648–2654.
115. Bacchetta, J., Cochat, P. and Salusky, I.B. (2011) [FGF23 and Klotho: the new cornerstones of phosphate/calcium metabolism]. *Arch. Pediatr.*, **18**, 686–695.
116. Kratz, O. (2004) The chemical laboratory: source of progress or chamber of horrors? *Angew. Chem. Int. Ed. Engl.*, **43**, 1770–1780.
117. Kratz, A., Ferraro, M., Sluss, P.M. and Lewandrowski, K.B. (2004) Laboratory reference value. *N. Engl. J. Med.*, **351**, 1548–1563.